Modulation of the *Pseudomonas aeruginosa* quorum sensing cascade by MexT-regulated factors

Andrew Frando[1], Robert S. Parsek[2], Jamal Omar[2], Nicole E. Smalley[1], Ajai A. Dandekar[1,2,*]

Departments of [1]Medicine and [2]Microbiology

University of Washington

Seattle, WA 98195 USA

Address correspondence to:

Ajai A. Dandekar

K-359A HSB, Box 356522

1705 NE Pacific St

Seattle, WA 98195

dandekar@uw.edu

Running title: Determinants of the *P. aeruginosa* QS hierarchy

Keywords: LasR, RhlR, PqsR, efflux, quorum sensing

1 Abstract

2 *Pseudomonas aeruginosa (Pa)* uses quorum sensing (QS), a cell-cell communication system

3 that enables it to sense cell density and to alter gene expression. *Pa* has three complete QS

4 circuits controlled by the regulators LasR, RhlR, and PqsR, that together activate hundreds of

5 genes. In the well-studied strain PAO1, QS is organized hierarchically, with PqsR and RhlR

6 activity dependent on LasR. This hierarchy depends on the non-QS transcription factor MexT;

7 deletion of *mexT* allows for RhlR activity in the absence of LasR. We aimed to identify how

8 MexT modulates the *Pa* QS architecture. We compared the transcriptome of PAO1 to that of

9 PAO1Δ*mexT* and determined a MexT regulon. We identified two MexT-regulated operons that

10 may affect the QS hierarchy: the efflux pump genes *mexEF-oprN* and the *Pseudomonas*

11 quinolone signal (PQS) synthesis genes *pqsABCDE*. We tested whether the products of these

12 genes affected the QS hierarchy. A *mexEF* knockout mutant, like a *mexT* deletion mutant,

13 exhibited RhlR activity earlier, and to a higher magnitude, than wild-type PAO1. MexEF-OprN is

14 known to export quinolones, and we found that exogenous addition of PQS, through PqsE, also

15 resulted in earlier and higher magnitude of RhlR activity compared to wild-type PAO1. We also

16 discovered alternate QS architectures in clinical isolates, where RhlR activity is not fully

17 dependent on LasR. In these isolates, surprisingly, MexT does not influence the relationship

18 between LasR and RhlR. Our work reveals a new suite of factors that regulate QS in *Pa*, with

19 implications for bacterial behaviors in environmental and clinical settings.

20   <u>Importance</u>

21   Bacteria interact with both abiotic and biotic factors in their environment. Quorum sensing (QS)

22   is one mechanism that bacteria use to communicate with other bacteria and coordinate

23   behaviors in the population. QS regulates a wide variety of processes ranging from the

24   production of light to modulation of virulence factors; some bacteria use single QS circuits, while

25   others have several. The opportunistic pathogen *Pseudomonas aeruginosa* uses QS to control

26   some virulence functions and has three complete QS circuits. Our study explores why bacteria

27   might have multiple QS circuits. We show how a non-QS transcription factor, MexT, influences

28   QS regulators in *P. aeruginosa* and we uncover the diversity of QS architectures in clinical

29   isolates. This study begins to reveal the benefits (or disadvantages) of multiple QS circuits,

30   allowing us to understand behaviors of bacteria that have a range of implications including in

31   health, agriculture, and bioremediation.

Introduction

32   Introduction

33   Bacteria can occupy a variety of environments that include the ocean, human body, and soil,

34   and seldom live in isolation. Bacteria have many methods of adapting to environmental changes

35   and interacting with other microbes, including by using various forms of signaling. Quorum

36   sensing (QS) is a type of intercellular communication used by many bacteria to coordinate

37   group behaviors in response to cell density. QS is a feature of many gram-positive and gram-

38   negative bacteria and typically results in transcription factor activation of gene expression (1).

39   Bacterial behaviors regulated by QS include the production of light, biofilm formation, and the

40   secretion of virulence factors.

41

42   QS is typically organized into circuits composed of a signal producing enzyme and a signal-

43   responsive transcriptional regulator. *Pseudomonas aeruginosa* (*Pa*) is a gram-negative

44   opportunistic bacterial pathogen that encodes multiple QS circuits that are controlled by the

45   transcriptional regulators LasR, RhlR, and PqsR (also called MvfR) (2). Together, the three QS

46   circuits regulate 5% of gene expression, including virulence factors like proteases, toxins, and

47   biofilm components (3).

48

49   LasR and RhlR are both QS transcription factors that respond to acyl-homoserine lactone (AHL)

50   signals (4). LasI produces the signal *N*-3-oxo-dodecanoyl homoserine lactone (3OC12-HSL)

51   that binds to and results in LasR activity. Similarly, RhlI produces the signal *N*-butanoyl

52   homoserine lactone (C4-HSL) that binds to RhlR. The PqsR QS circuit involves the quinolone

53   signals 2-heptyl-4-quinolone (HHQ) and 2-heptyl-3-hydroxy-4(1H)-quinolone (PQS) (5-8). In a

54   process different from AHL QS, HHQ and PQS are synthesized from multiple enzymes encoded

55   by *pqsABCD* and *pqsH*. All three circuits behave in a positive feedback loop where signals that

56   bind activate the transcriptional regulator, which in turn results in increased expression of the

57   signal synthase enzymes (9), a typical feature of QS circuits.

58

59   The interconnectivity between the QS circuits, or QS architecture, differs between *Pa* strains. In

60   the laboratory strain PAO1, QS architecture is hierarchical, where PqsR and RhlR expression

61   are dependent on LasR (10). A *lasR*-null strain in PAO1 is generally in a QS-off state (11). There

62   are additional layers of interaction: the chaperone PqsE, which is regulated by PQS QS, has

63   been shown to positively affect RhlR activity, while RhlR negatively regulates production of PQS

64   (12-14). The QS architecture in some clinical isolates seems to vary from PAO1. We and others

65   have found that despite encoding inactivating mutations in *lasR*, *Pa* clinical isolates derived from

66   chronic infections of people with cystic fibrosis are capable of activating RhlR QS independent

67   of LasR, in a manner that differs from PAO1 (15-17). The question remains whether these

68   clinical isolates have QS architectures that are fundamentally different from PAO1 or if the

69   phenotype is explained, instead, by mutations that were acquired in addition to those in *lasR*.

70

71   More recent work has identified how PAO1 can itself develop a LasR-independent QS

72   architecture. The "wildtype" strain PAO1 acquired a loss-of-function mutation in the

73   oxidoreductase gene *mexS*, presumably as a consequence of exposure to chloramphenicol (18-

74   20). MexS responds to oxidative stress and negatively regulates the activity of a transcriptional

75   regulator, MexT. Because of the inactivating mutation in *mexS,* MexT is constitutively active in

76   PAO1 and induces many genes including the RND drug efflux pump MexEF-OprN. MexEF-

77   OprN has been shown to influence QS, in part by delaying the activation of PQS QS (21).

78   Recent work has linked MexT to the regulation of QS in PAO1 (22-24). PAO1 with inactivating

79   mutations in *lasR* do not activate RhlR QS. However, *lasR* mutants exhibit RhlR activity if there

80   is also an inactivating mutation in the *mexT*. These data indicate that MexT contributes to the

81   LasR-dependent QS architecture in PAO1, but the mechanisms driving this phenomenon are

82   unknown.

83

84   We are interested in QS architectures and how they are regulated, with the idea that the

85   arrangement of QS circuits might impact bacterial virulence, social behaviors, or both. To

86   investigate this issue, we explored how MexT regulates QS in the laboratory strain PAO1. We

87   determined the MexT regulon by comparing the transcriptomes of wild-type PAO1 to a *mexT-*

88   null mutant*.* We ascertained that the efflux pump MexEF-OprN and the chaperone protein PqsE

89   both contribute to the LasR-dependent QS architecture in PAO1. To study the diversity of

90   quorum sensing architectures, we next explored QS architecture in clinical isolates with

91   functional LasR alleles. We identified isolates with a PAO1-like QS architecture where RhlR

92   activity is dependent, to varying degrees, on intact LasR, expanding the array of known QS

93   architectures in *Pa*. Finally, we determined that MexT did not influence QS architecture in some

94   of these clinical isolates, suggesting the existence of other regulators of the QS hierarchy in *Pa*.

95   Results

96   ***The MexT regulon***

97   Because inactivating mutations in *mexT* alter the QS hierarchy in PAO1, we started by exploring

98   how MexT regulates quorum sensing architecture in this strain. MexT is a transcription factor

99   that is known to regulate several genes (25, 26), although the full extent of its gene regulation is

100   not fully known, because a prior study compared the wild-type to an overexpression variant (26),

101   and we now understand that MexT is constitutively expressed in PAO1. We aimed to identify

102   MexT-regulated genes that modulate QS, specifically components of the MexT regulon that

103   might impact the timing of RhlR QS.

104

105   We compared RhlR activity in a PAO1 *mexT* knockout mutant (PAO1Δ*mexT*), to that of wild-type

106   PAO1 (**Figure 1**). In agreement with prior studies (22, 23), we found that the PAO1Δ*mexT*

107   mutant exhibited higher RhlR activity at lower cell densities compared to wild-type. The

108   PAO1Δ*mexT* knockout mutant has robust RhlR activity as early as an OD_{600} of 1.0, while wild-

109   type PAO1 exhibits RhlR activity around an OD_{600} of 2.0. We identified the OD_{600} of 1.0 and 2.0

110   as the specific growth stages we would use to identify MexT-regulated genes that might
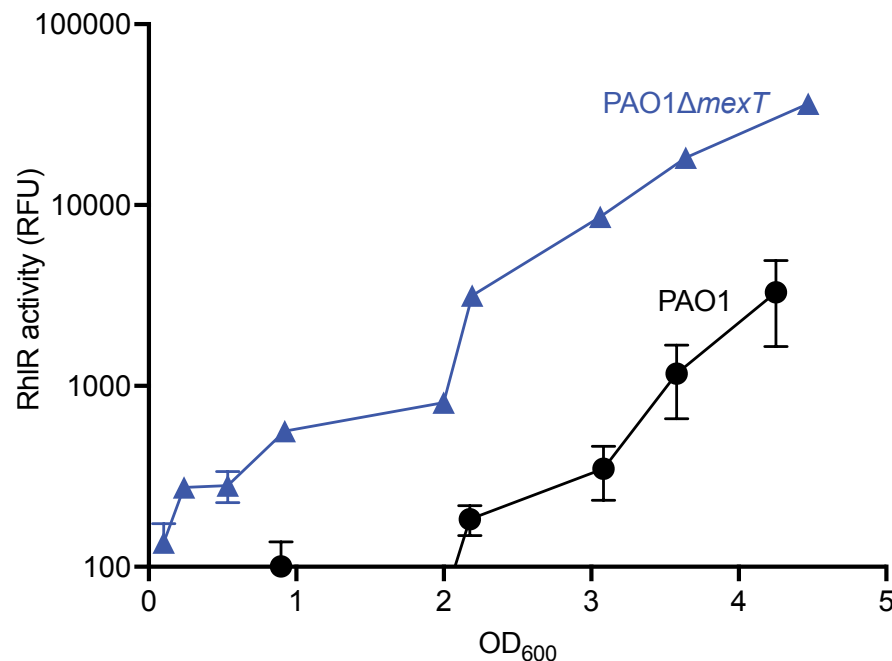
111   modulate RhlR QS.

112

Figure 1. **PAO1Δ*mexT* exhibits earlier and greater RhlR activity than the wild-type.** Wild-type PAO1

and PAO1Δ*mexT* were grown in flasks for 4.5 hours. Bacterial growth was determined by OD_{600}, and

RhlR activity was determined using a reporter plasmid with the promoter of the RhlR-regulated gene *rhlA*

controlling GFP expression. The x-axis shows OD_{600}, and the y-axis shows RhlR activity as measured

using the *rhlA-gfp* reporter plasmid.

118

We performed an RNA-sequencing experiment using wild-type PAO1 and a *mexT* knockout

mutant to identify differentially expressed genes (DEGs) at OD_{600} of 1.0 and 2.0. We compared

gene expression between the two strains using DESeq2 (27) and determined the MexT regulon.

We defined DEGs as genes in the *mexT* knockout mutant that have at least a 2-fold change

compared to wild-type PAO1 and a *p*-value < 0.05. In total, we identified 152 DEGs at an OD_{600}

of 1.0, with 104 genes exhibiting higher expression in the *mexT* knockout mutant and 48 genes

having higher expression in wild-type PAO1 (**Supplemental Table 1**). We identified 265 DEGs

at an OD_{600} of 2.0, with 178 genes showing higher expression in the *mexT* knockout mutant and

87 genes having higher expression in wild-type PAO1 (**Supplemental Table 2**). Based on this

8

128   experiment, the MexT regulon increases during growth. We observed 98 genes shared between

129   the regulon at an OD_{600} of 1.0 and 2.0, demonstrating that over 60% of genes at OD_{600} of 1.0

130   continued to be expressed and differentially regulated later in growth.

131

132   We observed that a PAO1Δ*mexT* mutant showed an earlier and higher magnitude of RhlR

133   activation, indicating that MexT likely negatively regulates RhlR in wild-type PAO1 (**Figure 1**).

134   Consistent with this observation, the transcriptomes we identified include several genes

135   regulated by RhlR. These genes are probably not contributing to MexT-specific regulation of

136   QS. Therefore, we filtered out genes that belong to the core RhlR regulon that was identified

137   previously using the laboratory strain PAO1 and clinical isolates derived from people with cystic

138   fibrosis (**Figure 2 and Table 1)** (15, 16, 28). Because there was robust RhlR activation at both

139   OD_{600} of 1.0 and 2.0, we focused on the OD_{600} 1.0 transcriptome for the remainder of our work,

140   since it was more likely to include factors relevant to RhlR regulation and fewer genes that are

141   activated by RhlR itself.

142

143   Using the OD_{600} 1.0 transcriptome, we identified 115 genes that belong solely to the MexT

144   regulon with 47 genes that appear to be activated by MexT (genes with lower expression in

145   PAO1Δ*mexT* compared to wild-type PAO1) and 68 genes that appear to be repressed (genes

146   with higher expression in PAO1Δ*mexT* compared to wild-type PAO1). Within the MexT regulon,

147   we identified 51 genes that were identified in the previous study that used a MexT

148   overexpression mutant (25). In total, over 30% of the genes identified in the prior study were

149   identified in ours. The genes we identified in the MexT regulon at an OD_{600} of 1.0 belong to

150   several protein families, including transporters, phenazine biosynthesis, and transcriptional
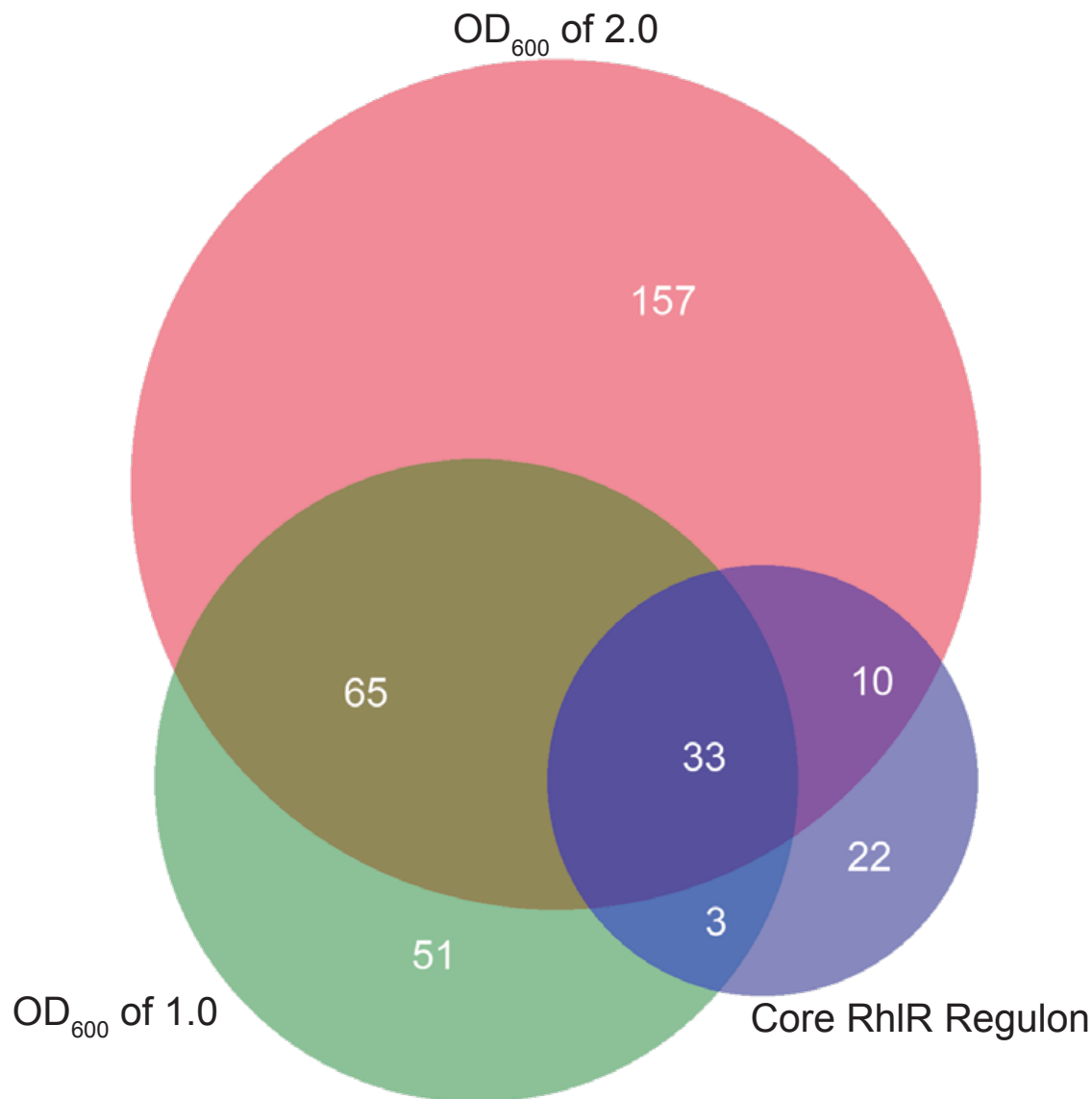
151   regulators.

152

9

153

Figure 2. **The MexT regulon encompasses at least 150 genes and overlaps with the RhlR regulon**.

Venn diagram showing the overlap of genes between an OD_{600} of 1.0 and 2.0, and a previously identified

RhlR regulon (15, 16, 28).

157

To identify MexT effectors that might modulate QS, we filtered for genes that have a high

confidence, such as those exhibiting large fold-changes, identification of whole operons, and

genes with known QS interactions. Our data validate other studies showing that MexT is a

transcriptional regulator of the multidrug RND efflux pump MexEF-OprN (26, 29). MexEF-OprN

162   is known for transport of the quorum sensing signal HHQ, a PQS precursor molecule, resulting

163   in delayed PQS QS (21). A recent study screening for QS-inhibitory compounds identified Z-

164   ethylthio enynone as a molecule that targets MexEF-OprN and affects C4-HSL concentrations

165   intra- and extracellularly in wild type PAO1 (30). Given these facts, it is plausible that MexEF-

166   OprN expression is induced by constitutive MexT activity and modulates quorum sensing

167   architecture by altering QS signal concentrations and affecting QS activation.

168

Gene expression changes in PAO1Δ*mexT* compared to PAO1								
Gene	$\log_2$ fold-change	p-value	Gene	$\log_2$ fold-change	p-value	Gene	$\log_2$ fold-change	p-value
PA4881	-6.5	6.71E-30	PA2811	-1.3	9.80E-17	opdC	1.3	4.27E-16
mexF	-6.4	<1.0E-40	PA2358	-1.3	2.19E-02	opmD	1.3	1.46E-04
mexE	-6.3	<1.0E-40	pagL	-1.2	1.78E-20	kdpB	1.3	1.44E-05
PA3229	-6.1	<1.0E-40	PA2812	-1.2	3.53E-07	pqsA	1.4	3.63E-15
PA1942	-6.0	<1.0E-40	nosL	-1.2	6.82E-04	stp1	1.4	3.19E-06
oprN	-6.0	<1.0E-40	PA3283	-1.1	9.10E-05	pqsC	1.4	1.19E-05
PA4623	-5.8	<1.0E-40	PA2354	-1.1	1.65E-03	mexH	1.4	3.65E-07
PA1744	-4.6	<1.0E-40	bexR	-1.1	4.11E-12	ladS	1.4	5.18E-26
PA2486	-4.5	<1.0E-40	PA1418	-1.1	1.70E-02	pqsB	1.4	1.64E-07
PA1743	-4.2	<1.0E-40	chiC	1.0	1.19E-03	pscF	1.4	1.05E-03
PA3871	-3.8	6.57E-05	PA1658	1.0	3.37E-02	PA1669	1.4	4.88E-11
PA4354	-3.8	<1.0E-40	pchA	1.0	8.82E-04	PA1668	1.4	8.81E-07
narI	-3.8	5.45E-05	oprB	1.0	1.77E-08	pchE	1.4	4.11E-12
PA2487	-3.7	<1.0E-40	phzS	1.0	5.93E-04	phzD2	1.4	5.31E-04
narJ	-3.7	3.32E-04	PA2097	1.0	1.21E-02	phnA	1.4	7.42E-10
moaA1	-3.6	4.17E-05	PA2362	1.1	3.20E-02	rbsC	1.5	3.19E-06
PA2485	-3.5	<1.0E-40	PA3377	1.1	2.71E-03	PA2782	1.5	4.88E-05
PA1970	-3.5	<1.0E-40	PA4341	1.1	3.22E-02	PA2068	1.5	1.44E-05
PA3230	-3.2	<1.0E-40	phzE2	1.1	3.10E-04	PA3574a	1.5	5.04E-03
PA4355	-2.9	1.10E-29	bkdA1	1.1	1.50E-02	PA2067	1.6	3.12E-03
narH	-2.7	2.04E-05	pscE	1.1	7.13E-03	hcpA	1.6	5.93E-06
gbuA	-2.6	2.06E-14	PA4219	1.1	1.01E-03	PA2781	1.6	4.08E-08
PA1333	-2.6	1.20E-24	kdpC	1.1	3.09E-02	rbsA	1.6	1.21E-03
PA2813	-2.5	<1.0E-40	PA3677	1.1	1.19E-03	PA4142	1.7	3.10E-14
xenB	-2.4	3.19E-21	stk1	1.2	1.09E-06	hcpB	1.7	5.57E-06
nosY	-2.2	2.17E-04	PA1657	1.2	5.06E-03	pchF	1.7	5.28E-04
PA2491	-2.2	<1.0E-40	pchD	1.2	4.78E-04	PA2260	1.8	1.49E-07
PA1419	-2.1	1.04E-09	phzF2	1.2	1.57E-03	pchC	1.8	1.49E-07
nirN	-2.1	5.30E-06	pqsD	1.2	1.05E-04	hisJ	1.8	1.55E-02
PA0510	-2.1	1.17E-08	hcpC	1.2	1.42E-03	pchB	1.8	1.48E-07
PA2759	-2.0	2.58E-30	PA0050	1.2	6.64E-05	PA3519	1.8	7.49E-03
PA4882	-2.0	7.54E-35	PA2322	1.2	1.09E-03	PA4596	1.8	1.56E-02
PA1420	-1.9	1.30E-14	popN	1.3	3.56E-04	PA2069	1.8	1.18E-11
PA3381	-1.7	5.26E-03	bkdA2	1.3	5.90E-10	oprD	1.9	2.63E-27
PA1417	-1.6	3.35E-06	hpcG	1.3	1.58E-12	PA3325	2.0	1.37E-25
PA2758	-1.6	5.48E-22	PA5180	1.3	1.19E-03	PA5328	2.2	1.60E-02
PA3282	-1.5	3.62E-04	pqsE	1.3	1.19E-05	pcrG	2.2	1.28E-04
PA1416	-1.5	5.77E-06	PA4218	1.3	2.23E-05	PA0165	2.3	7.90E-33
						PA4133	2.7	1.12E-27

169

Table 1. **The MexT regulon**. We performed RNA-seq on wild-type PAO1 and PAO1Δ*mexT* grown to an OD$_{600}$ of 1.0. Differentially expressed genes are defined as genes that showed a 2-fold change compared to wild-type PAO1 and had a p-value less than 0.05. We further filtered the differentially expressed genes to exclude those that belong to the core RhlR regulon.

12

174 ***MexT regulation of efflux pumps affects the QS hierarchy.***

175 We explored the role of MexEF-OprN in modulating QS in PAO1. We hypothesized that, like

176 MexT, MexEF-OprN negatively regulates RhlR activity. To test this, we first made a *mexEF*

177 knockout mutant to disrupt the efflux activity of MexEF-OprN. Like other RND systems found in

178 *P. aeruginosa*, membrane transport of substrates requires all three proteins to function (31).

179 We then introduced episomal plasmids with reporters for LasR (*lasI-gfp*), RhlR (*rhlA-gfp*), or

180 PqsR (*pqsA-gfp*) activity. We engineered a *mexEF* knockout mutant, which is sufficient to

181 disrupt the efflux pump since it needs all three proteins to function, and introduced these QS

182 reporter plasmids. The *mexEF* knockout mutant shows similar LasR activity and timing

183 compared to wild-type PAO1 and the *mexT* knockout mutant (**Figure 3A**). However, RhlR

184 activity was different: we observed that the *mexEF* knockout mutant, like PAO1Δ*mexT*, showed

185 earlier and higher RhlR activity compared to wild-type PAO1 (**Figure 3B**). This finding

186 demonstrates that the efflux pump MexEF-OprN is an important MexT-regulated effector

187 modulating QS. Further, we found PqsR activity earlier in both the *mexT* and *mexEF* knockout

188 mutants. In parallel, we tested the role of MexEF-OprN in regulating RhlR QS by creating an

189 integrating plasmid that contains *mexEF-oprN* under the control of an arabinose-inducible

190 promoter (PAO1 + *mexEF-oprN* OE) and compared this mutant to wild-type and PAO1Δ*mexT*

191 (**Figure 3D**). When we induced expression of *mexEF-oprN,* we found that the pump alters the

192 magnitude but not the timing of RhlR activation compared to PAO1 and PAO1 *mexEF-oprN* OE

193 without arabinose. These results corroborate the idea that MexEF-OprN impacts RhlR QS.

194 Together, they demonstrate that both *mexT* and *mexEF* knockout mutants affect RhlR and PqsR

195 QS. Because PAO1Δ*mexEF* phenocopies PAO1Δ*mexT*, it shows that MexT regulation of RhlR

196 QS acts at least in part through the efflux pump MexEF-OprN, indicating a regulatory pathway

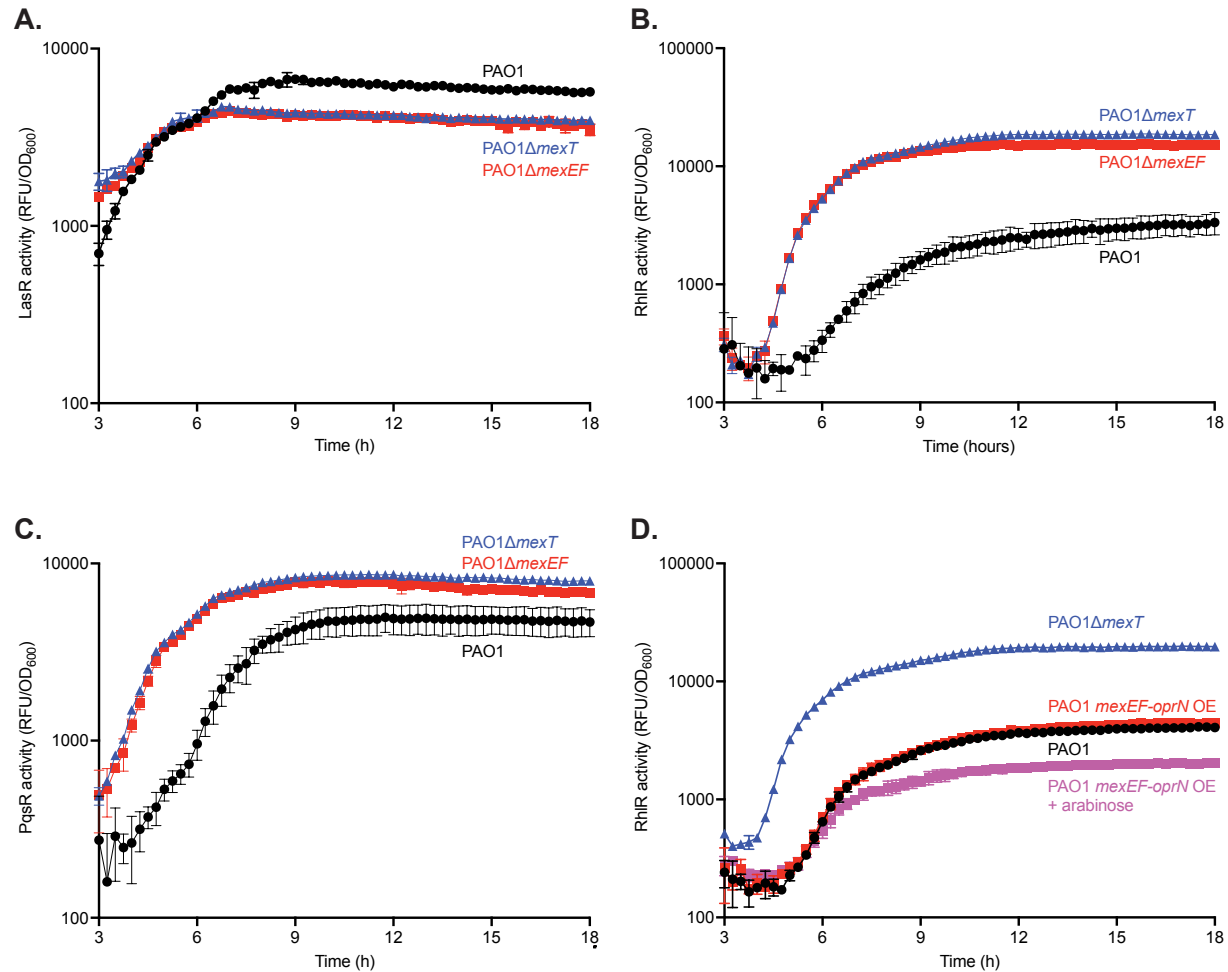197 from MexT to MexEF-OprN to RhlR QS.

198

Figure 3. **MexEF-OprN regulates both RhlR and PqsR QS**. **A**. LasR activity of PAO1, PAO1Δ*mexT*, and PAO1Δ*mexEF* were determined using a LasR activity (*lasI-gfp*) reporter plasmid. **B**. RhlR activity for PAO1, PAO1Δ*mexT*, and PAO1Δ*mexEF* were determined using a RhlR activity (*rhlA-gfp*) reporter plasmid. **C**. PqsR activity for PAO1, PAO1Δ*mexT*, and PAO1Δ*mexEF* were determined using a PqsR activity (*pqsA-gfp*) reporter plasmid. **D.** RhlR activity for PAO1, PAO1Δ*mexT*, PAO1Δ*mexEF*, and PAO1 + *mexEF-oprN* OE were determined using a RhlR activity reporter plasmid.

While RhlR activity is negatively regulated by MexEF-OprN and MexT in wild-type PAO1, RhlR activity eventually occurs during later growth phases, indicating that either the negative regulation is relaxed or a positive regulatory pathway is induced. To determine whether *mexEF-oprN* expression decreases over growth and leads to the increase in RhlR activity, we

14

211   performed a quantitative real-time PCR experiment to monitor *mexE* expression over bacterial

212   growth, with each subsequent timepoint compared to time 0 (**Figure 4A**). We observed that

213   *mexE* expression slightly increased at an OD_{600} of 1.0 and then further increased by more than

214   10-fold at an OD_{600} of 2.0. These results show that the increase in RhlR activity in PAO1 at later

215   time points is not driven by a reduction in *mexEF-oprN* expression.

216

217   We also tested whether the delay in RhlR activity in wild-type PAO1 was due to MexEF-OprN

218   modulating production of the RhlR signal C4-HSL. If C4-HSL is a substrate of MexEF-OprN, and

219   MexEF-OprN delayed RhlR QS by exporting C4-HSL signal, then we would expect a higher

220   extracellular C4-HSL concentration in wild-type PAO1 than in a *mexEF* deletion mutant. We

221   tested this hypothesis by measuring C4-HSL concentrations in wild-type PAO1 and

222   PAO1Δ*mexEF* over time (**Figure 4B**). We observed that total (cellular + supernatant) and

223   extracellular (supernatant only) C4-HSL concentrations were similar between wild-type PAO1

224   and PAO1Δ*mexEF* at OD_{600} of 0.3. At an OD_{600} of 0.8 and 2.0, we observed activation of RhlR in

225   the PAO1Δ*mexEF* mutant, evidenced by the increase in both total and extracellular C4-HSL

226   concentrations. (**Figure 2**). Importantly, we do not observe any differences between total and

227   extracellular C4-HSL concentrations in wild-type PAO1 or PAO1Δ*mexEF* at any point in growth,

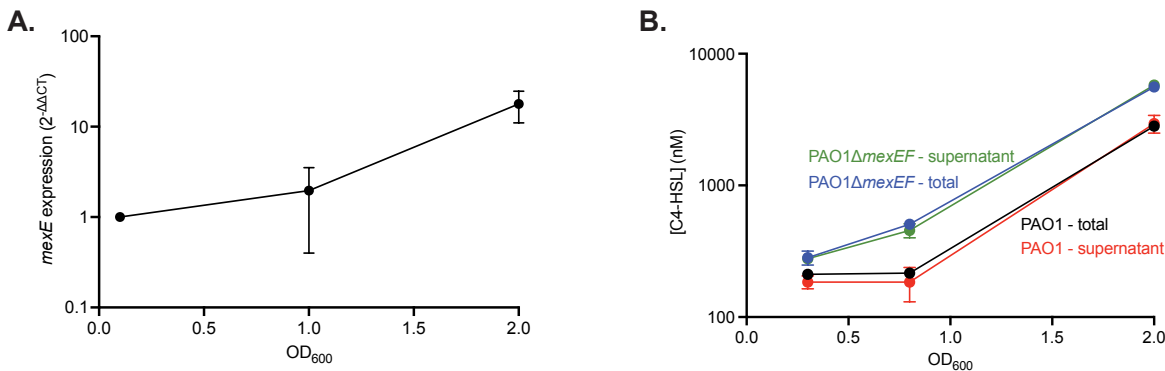228   indicating that MexEF-OprN is not altering C4-HSL concentrations in a way that could alter RhlR

229   activity.

15

230

231

232 **Figure 4. Expression of *mexEF-oprN* and C4-HSL concentrations do not account for changes in**

233 **RhlR activity. A**. Quantitative real-time PCR measuring *mexE* transcripts during bacterial growth of wild-

234 type PAO1. *mexE* expression was normalized to *rplU* and reported as $2^{-\Delta\Delta CT}$. **B**. C4-HSL was extracted

235 from total cultures and culture supernatant over bacterial growth. C4-HSL concentrations were

236 determined using a previously described *E. coli* reporter.

237

238 ***MexT regulation of PqsE also contributes to the QS hierarchy***

239 MexEF-OprN has been shown to delay PQS QS through binding and exporting the PQS

240 precursor HHQ (21). The gene product of *pqsE*, which is regulated by PQS QS, is known to

241 interface with Rhl QS by positively regulating activation of some genes in the RhlR regulon (32,

242 33). We observed that the MexT regulon at an OD_{600} of 1.0 included the entire PQS

243 biosynthesis operon *pqsABCDE,* which includes the gene encoding the chaperone PqsE.

244 Because we identified these PQS biosynthesis genes in our RNA-seq experiment and have

245 shown a role of MexEF-OprN in regulating RhlR QS, we hypothesized that constitutive MexT

246 activity induces *mexEF-oprN* expression, leading to repression of PQS QS, delayed *pqsE*

247 expression, and thus delaying RhlR activation.

248

249 We tested whether MexT delays PQS QS through the MexEF-OprN efflux pump. We measured

250 PqsR activity in wild-type PAO1 supplemented with exogenous PQS and compared that to the

16

251 PAO1Δ*mexT* and PAO1Δ*mexEF* mutants (**Figure 5A**). We found that addition of exogenous

252 PQS to the wild-type culture phenocopies the PqsR activity we observed in both PAO1Δ*mexT*

253 and PAO1Δ*mexEF*, demonstrating that the delay in PQS activity in wild-type PAO1 can be

254 attributed to the regulatory activity of MexT and MexEF-OprN.

255

256 We next determined whether this delay in PQS QS affected RhlR QS. We measured RhlR

257 activity in PAO1Δ*mexT* and PAO1Δ*mexEF*, and we reasoned that addition of exogenous PQS

258 may alter RhlR activity to match that of the PAO1Δ*mexT* and PAO1Δ*mexEF* mutants, like PqsR

259 activity (**Figure 5B**). We found that the addition of exogenous PQS did indeed result in earlier

260 and higher RhlR activity compared to wild-type PAO1. However, the activity was intermediate

261 between wild-type PAO1 and both PAO1Δ*mexT* and PAO1Δ*mexEF*, indicating that the delay in

262 PQS QS only partially accounts for the relative delay of RhlR QS in wild-type PAO1.

263

264 Because we observed a change in RhlR activity with the addition of PQS, we sought to identify

265 the factor mediating this change. PqsE is known to act as a chaperone and activate RhlR.

266 Further, based on our transcriptome data, we observed higher expression of *pqsE* in the

267 PAO1Δ*mexT* mutant compared to wild-type PAO1. Together, these data led us to speculate that

268 the regulation of RhlR activity in wild-type PAO1 was due to repression of *pqsE*. To test this

269 hypothesis, we constructed a mutant to counter *pqsE* repression mediated by MexT. This

270 mutant contains an integrated plasmid with *pqsE* under the control of an arabinose-inducible

271 promoter (PAO1 + *pqsE* OE), and we compared RhlR activity in this mutant to wild-type PAO1,

272 PAO1Δ*mexT*, and PAO1Δ*mexEF* (**Figure 5B**). We found that PAO1 + *pqsE* OE without

273 arabinose showed similar RhlR activity as wild-type PAO1, indicating negligible basal

274 expression from the promoter. However, with the addition of arabinose, PAO1 + *pqsE* OE

275 showed nearly identical RhlR activity to wild-type supplemented with exogenous PQS.

276

17

277   We further assessed the role of PqsE by creating a *mexT* and *pqsE* double knockout mutant

278   (PAO1Δ*mexT*Δ*pqsE*) and compared RhlR activity in this mutant to wild-type PAO1 and

279   PAO1Δ*mexT* (**Figure 5C**). In agreement with the prior experiment, we observed a decrease in

280   RhlR activity that occurred at a slightly later timepoint in PAO1Δ*mexT*Δ*pqsE* compared to

281   PAO1Δ*mexT*. However, PAO1Δ*mexT*Δ*pqsE* retained higher RhlR activity compared to PAO1,

282   indicating that *pqsE* is necessary but not sufficient for MexT- and MexEF-OprN-mediated

283   regulation of RhlR activity. These experiments showed that the increase in RhlR activity due to

284   the addition of PQS is likely mediated by the earlier activation of PQS QS and increased
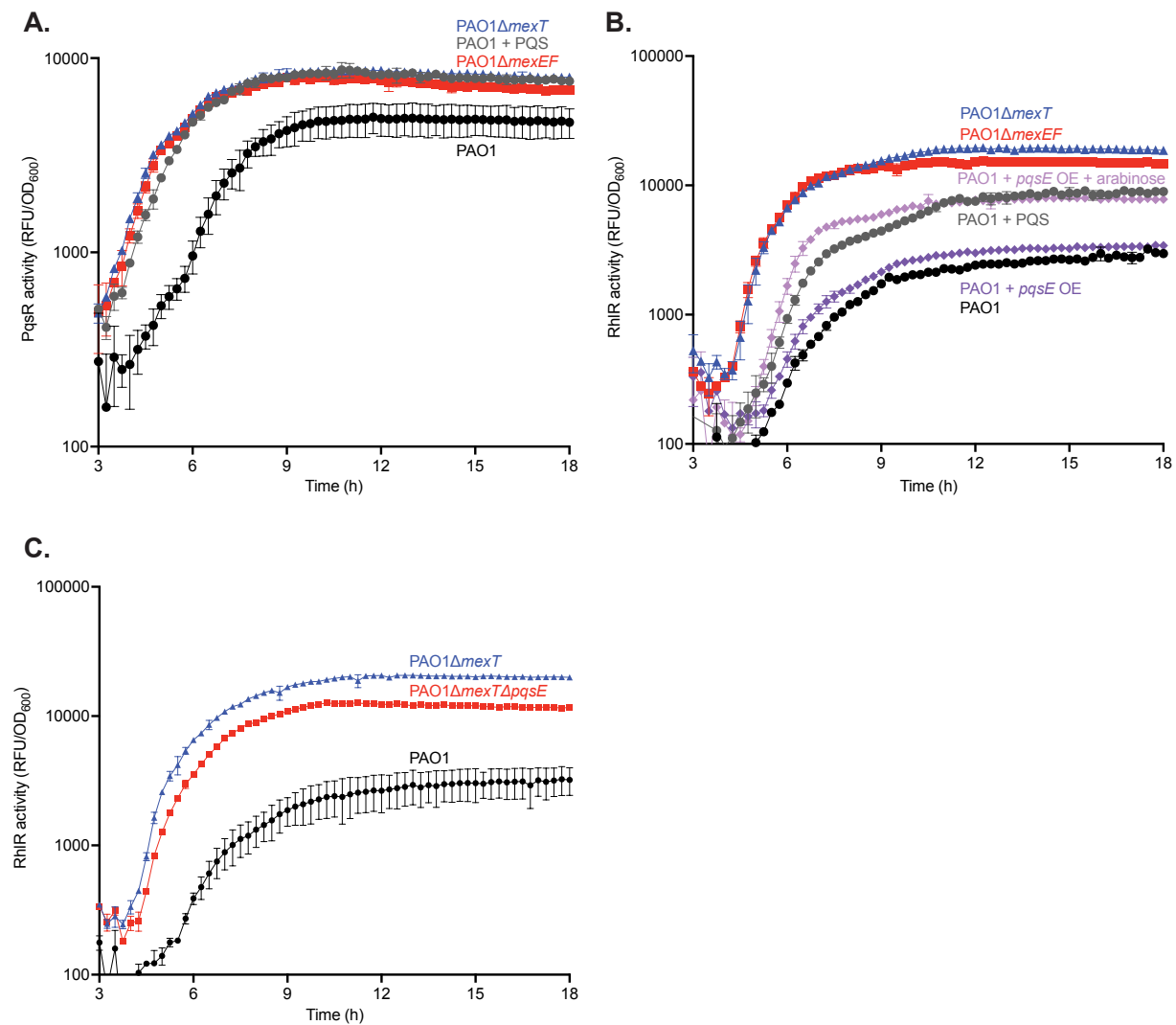
285   production of PqsE.

286

Figure 5. **PqsE partially regulates RhlR activity. A**. PqsR activity with and without addition of 20 μM PQS for PAO1, PAO1Δ*mexT*, and PAO1Δ*mexEF* was determined using a PqsR activity reporter plasmid. **B**. RhlR activity with and without addition of 20 μM PQS for PAO1, PAO1Δ*mexT*, PAO1Δ*mexEF*, and PAO1 + *pqsE* with and without arabinose were determined using a RhlR activity reporter plasmid. **C**. RhlR activity for PAO1, PAO1Δ*mexT*, PAO1Δ*mexT*Δ*pqsE* were determined using a RhlR activity reporter plasmid.

19

295 Together, these data enhance prior work on MexT, MexEF-OprN, and RhlR QS (**Figure 6**). We

296 showed that constitutive MexT activity in PAO1 resulted in increased expression of efflux pump

297 genes *mexEF-oprN*. At lower cell densities, the MexEF-OprN activity repressed RhlR activity.

298 This is partially mediated by the delay in both PQS activation and the production of PqsE that

299 would normally activate RhlR. There is an unidentified product regulated by MexEF-OprN that

300 further represses RhlR activity. At higher cell densities, LasR activity counteracts the repression

301 by MexEF-OprN and results in *rhlI/rhlR* and *pqsR* expression, leading to RhlR activity.

302

303 **Figure 6. MexT negatively regulates RhlR activity, while LasR positively regulates *rhlR***

304 **expression.** Cartoon showing the model of proposed MexT-mediated regulation of RhlR. At

305 lower cell density, MexT positively regulates *mexEF-oprN*, delaying PQS QS and *pqsE*

306 expression, and results in less active RhlR. At higher cell densities, LasR activity results in *rhlR*

307 expression and an increase in RhlR activity.

308

309

310

311 ***MexT is not the sole factor affecting QS architectures in P. aeruginosa***

312 We wondered about the diversity of quorum sensing architectures and their regulation in other

313 *P. aeruginosa* isolates. Recent work has identified clinical isolates that exhibit LasR-independent

314 RhlR QS, but these had *lasR* null mutations at the times of isolation. It is possible that other

315 mutations (such as in *mexT*) resulted in LasR-independent RhlR QS in these clinical isolates.

316 We queried whether the LasR-dependent hierarchy was present in other isolates. We reasoned

317 that if we knockout *lasR* in clinical isolates and RhlR activity is maintained, then these isolates

318 encode a QS architecture different from PAO1. However, if we knockout *lasR* in clinical isolates

319 and RhlR activity is abrogated, then the isolates display QS architecture akin to PAO1.

320

321 We started by assessing LasR and RhlR kinetics in three clinical isolates from chronic infections

322 in people with cystic fibrosis (E192, E194, and E195) (17). These are isolates from the Early

323 *Pseudomonas* Infection Control (EPIC) study (34) and harbor functional LasR proteins. Each

324 isolate was transformed with the LasR and RhlR reporter plasmids described earlier and

325 compared to wild-type PAO1 (**Figure 7**). All clinical isolates had active LasR QS that was similar

326 to PAO1. In contrast, RhlR activity occurred earlier in all clinical isolates compared to PAO1. All

327 three isolates exhibited at least 5-fold higher RhlR activity compared to PAO1. Together, these

328 data show that the clinical isolates exhibit differences in QS compared to PAO1, possibly
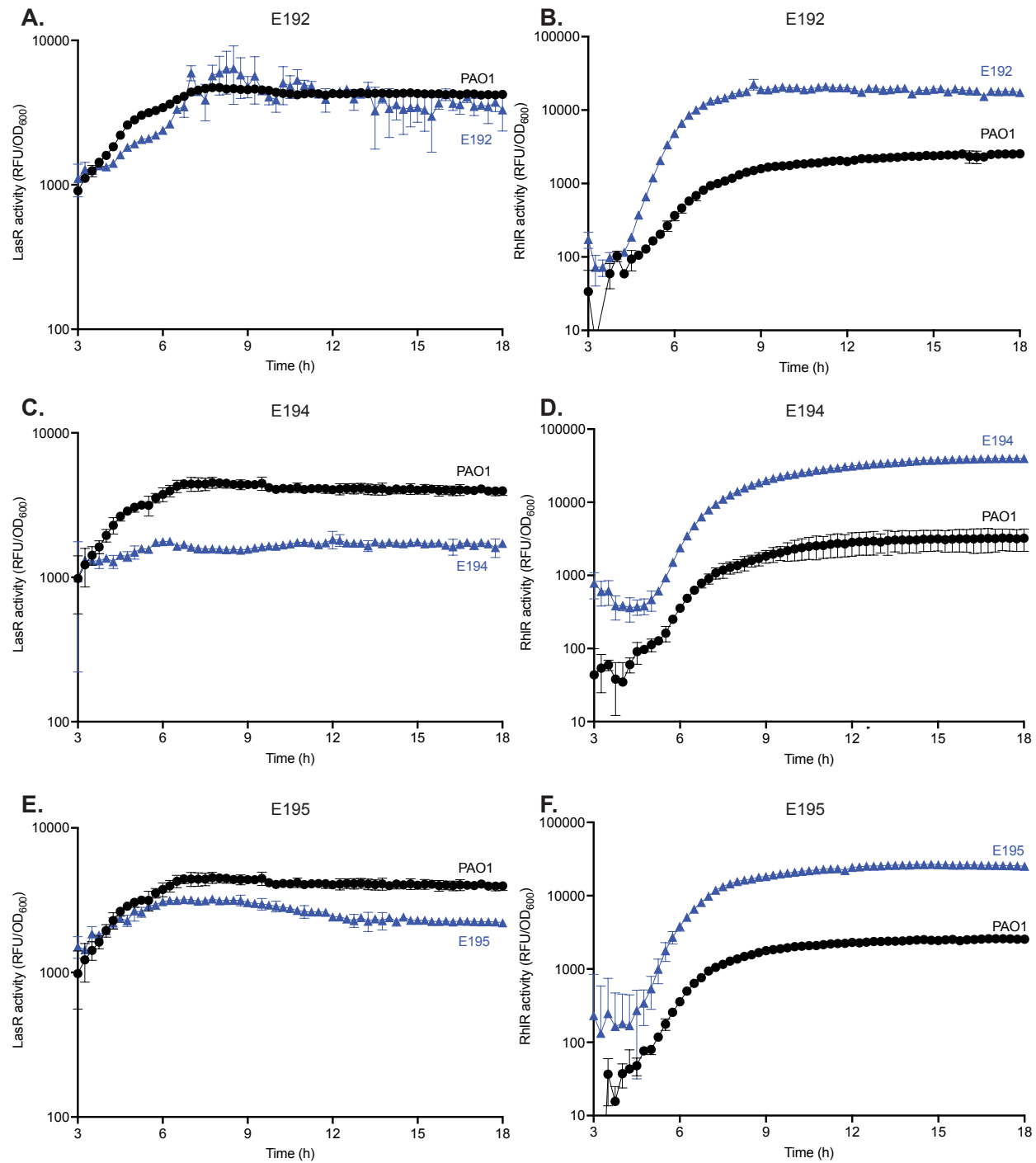
329 reflecting differences in QS architecture.

Figure 7. RhlR, but not LasR, activity is different between PAO1 and EPIC isolates. LasR activity for PAO1 compared to E192 (**A**), E194 (**C**), and E195 (**E**), measured using a LasR activity reporter plasmid. RhlR activity for PAO1 compared to E192 (**B**), E194 (**D**), and E195 (**F**), measured using a RhlR activity reporter plasmid.

22

335

336   We compared the QS architecture of clinical isolates to that of PAO1 by generating *lasR*

337   deletion mutants and measuring RhlR activity (**Figure 8**). In all clinical isolates, RhlR activity

338   occurred later and at a lower magnitude with *lasR* deletion compared to the parent (**Figure**

339   **8BCD**). However, clinical isolates still retained some RhlR activity, which differs from PAO1. Of

340   the three isolates, E195Δ*lasR* retained the most RhlR activity. For isolates E192 and E194,

341   RhlR activation in *lasR* mutants followed a linear pattern. For isolate E195, we observed RhlR

342   activation in the *lasR* knockout followed an S-curve pattern similar to wild-type PAO1 and the

343   parental strains.

344

345   We next assessed whether the variability of LasR-dependence was due to MexT modulation of

346   QS architecture. To ask this question, we performed whole genome sequencing on each clinical

347   isolate to identify changes in the overall genome compared to PAO1. Each isolate encodes a

348   larger genome than wild-type PAO1, ranging from 50 kbp to 600 kbp larger. E194 and E195

349   have identical *mexT* sequences to PAO1. E192 contained non-synonymous mutations that

350   resulted in an I298F and D302E variant. We also assessed the MexT regulator, MexS, that is

351   shown to be inactive in PAO1 due to a N249D mutation. In contrast to PAO1, all clinical isolates

352   encode N249, indicating each has a functional MexS protein.

353

354   To investigate MexT activity in the clinical isolates, we transformed each isolate with a MexT

355   reporter that contains the promoter of *mexE*, cloned upstream of *gfp* in an episomal plasmid.

356   Compared to wild-type PAO1, MexT activity in each clinical isolate was almost undetectable

357   (**Supplemental Figure 1**). MexT is activated due to oxidative stress, and others have

358   demonstrated that the chemical compound diamide induces oxidative stress and activates MexT

359   (22). PAO1 has constitutive MexT activity, but we observed a slight increase in MexT activity

360   with the addition of diamide. In contrast, with the addition of diamide to each clinical isolate, we

361   observed activation of MexT, indicating that MexT in each clinical isolate is functional, including

362   the double variant encoded in E192.

363

364   We next determined if RhlR activity in the clinical isolates was modulated by MexT (as it is in

365   PAO1) by generating *mexT* knockout mutants in each isolate and measuring RhlR activity

366   (**Figure 8**). E192Δ*mexT* and E195Δ*mexT* displayed no differences in RhlR activity compared to

367   wild-type isolates. Interestingly, E194Δ*mexT* showed earlier RhlR activity with the same terminal

368   intensity compared to wild-type E194. Altogether, the clinical isolates differ from PAO1: the

369   absence of MexT does not substantially change RhlR activity in *mexT* knockout mutants.

370

371   We asked whether MexT affects the relationship between LasR and RhlR QS. In PAO1, we

372   observed an increase in RhlR QS in PAO1Δ*lasR*Δ*mexT* compared to PAO1Δ*lasR* (**Figure 8A**).

373   In contrast, each clinical isolate exhibited no change in RhlR activity when comparing *lasR*

374   knockout mutants to *lasR* and *mexT* double knockout mutants (**Figure 8BCD**). Together these

375   results indicate that while the clinical isolates depend on LasR for RhlR activity, their RhlR

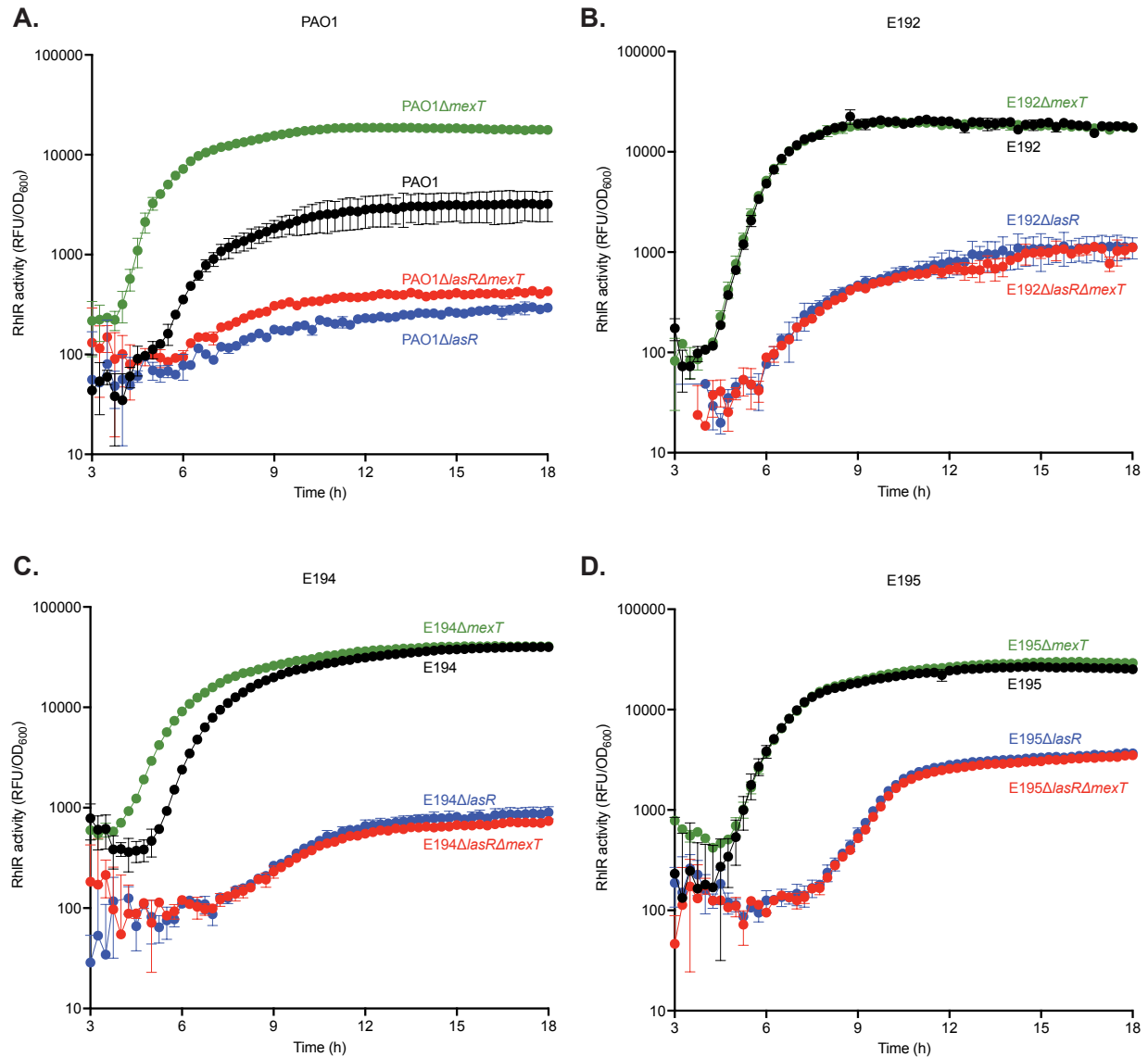376   activity is not negatively regulated by MexT as it is in PAO1.

Figure 8. **EPIC isolates exhibit LasR-dependent but MexT-independent RhlR activity.** RhlR activity for wild-type, *lasR* and *mexT* knockouts*,* and *lasR* - *mexT* double knockout mutants for PAO1 (**A**), E192 (**B**), E194 (**C**), and E195 (**D**) measured using a RhlR activity reporter plasmid.

Discussion

In this work, we explored QS architectures in laboratory and clinical isolates of *P. aeruginosa* and how these architectures are modulated. We investigated how the transcription factor MexT promotes a LasR-dependent quorum sensing architecture in the laboratory strain PAO1 through

25

386   bacterial genetics and transcriptomics. We discovered that the MexT-regulated genes *mexE,*

387   *mexF*, and *oprN*, contribute to QS architecture. When these are inactivated, there is an increase

388   in RhlR activity compared to the wild-type. Further, MexEF-OprN enforces this architecture

389   through regulation of PQS QS and PqsE. By assessing the diversity of quorum sensing

390   architecture across *P. aeruginosa*, we discovered that the QS hierarchy in a subset of clinical

391   isolates from chronic infections of people with cystic fibrosis are LasR-dependent, but the

392   degree of dependence varies across isolates, with none exhibiting absolute LasR dependence.

393   Finally, we found that while there is LasR-dependent RhlR QS, in some isolates it was not

394   dependent on MexT activity, demonstrating that the clinical isolates had a similar architecture

395   but may depend on a modulator other than MexT.

396

397   Our study identifies the mechanism of a key regulator of QS in *P. aeruginosa*. We originally

398   hypothesized that QS regulation was mediated either by the efflux pump MexEF-OprN or the

399   chaperone PqsE. However, our data suggests it is the combination of both – induction of

400   *mexEF-oprN* expression and repression of *pqsE* expression – that drives the LasR-dependent

401   RhlR QS observed in strain PAO1. Several other studies have identified the QS signals C4-

402   HSL, 3OC12-HSL, and HHQ as potential or established substrates of the efflux pump MexEF-

403   OprN, supporting our finding that MexEF-OprN regulates QS (21, 30). Separate studies have

404   shown that a suite of RhlR-regulated genes requires PqsE (32, 33). Our study shows a

405   synergistic role between the two in regulating the *Pa* QS architecture, and we identified two

406   potential mechanisms by which this happens. Further, our study reveals that RhlR-regulation by

407   MexEF-OprN is also modulated by a PqsE-independent pathway. We are exploring potential

408   candidates in a PqsE-independent pathway by examining the MexT regulon we identified in this

409   study.

410

411   Our laboratory and others have characterized QS extensively in strain PAO1 (2, 3, 23, 35), but

412   we wanted to further explore the diversity of QS architectures. We previously identified LasR-

413   independent QS in clinical isolates derived from chronic infections of people with cystic fibrosis

414   (15). However, these isolates harbored *lasR* null mutations at the time of isolation, and it was

415   unknown if these isolates developed a different architecture from PAO1 due to other genomic

416   differences. We showed in this study that clinical isolates can also have LasR-dependent QS,

417   like PAO1. Surprisingly, we observed varying degrees of dependence on LasR, ranging from

418   complete dependence on LasR for RhlR activity in E194 and partial dependence on LasR for

419   RhlR activity in E195. It will be of interest to explore the genetic differences between the strains

420   that result in differing degrees of dependence on LasR. Interestingly, while there was

421   dependence on LasR for RhlR activity in all clinical isolates, we discovered that this was not

422   dependent on MexT. This result illustrates that while PAO1 and clinical isolates share a similar

423   quorum sensing architecture, the modulators seem to be different. Identifying these other

424   modulators in the clinical isolates might illuminate the determinants of alternate QS

425   architectures.

426

427   Our study of MexT-mediated regulation of QS affords us some insight into the formation of QS

428   hierarchies. Some bacteria contain only a single QS circuit, while others have many (2, 36, 37).

429   Our study begins to explore the purpose of having multiple QS circuits, through understanding

430   how MexT functions to regulate QS. We also identified unique QS architectures in the EPIC

431   isolates, indicating different regulators may be required for particular environments. MexT may

432   have importance in the case of wound infections, where PAO1 was initially isolated, but it may

433   be dispensable in the airways from which the EPIC isolates were obtained.

434

435   This work also offers insight into the plasticity of the interactions between QS circuits and how

436   key regulators like MexT can alter QS architecture based on selective pressures and promote

437   architectures that might be advantageous in specific environments. Further, by studying and

438   identifying variants in regulators like MexT, we gain insight into how cooperative behaviors may

439   function within and between individuals. It is easy to imagine that regulatory mutants can

440   change QS architectures and cellular behaviors to allow for specialization within a community.

441   For example, a *mexT* mutant may arise when RhlR activity is required early, while the wild-type

442   defers the cost associated with RhlR QS, which might be advantageous when nutrients or other

443   resources are limited.

444

445   Altogether, our study defined the regulation of a key modulator of *P. aeruginosa* growth and

446   pathogenesis. By understanding how MexT modulates QS architecture, we begin to understand

447   how bacterial sociality is controlled. These results have implications and applications that

448   expand beyond bacterial pathogenesis and clinical settings. For example, how did MexT evolve

449   to regulate quorum sensing architecture in PAO1, but not the clinical isolates? What selective

450   factors favored genetic changes that resulted in LasR-dependent quorum sensing with different

451   architecture regulators? Do the environment and other microbial interactions affect which

452   architectures evolved (and which are beneficial in a given environment)? Our work pries the

453   door open on understanding, where QS differs by interaction and environment, what the

454   modulators of these QS architectures are.

455

456   <u>Materials and Methods</u>

457   **Bacteria and growth conditions.** Strains and plasmids used in this study are listed in

458   **Supplemental Tables 3 and 4.** *P. aeruginosa* was grown in lysogeny broth (LB) buffered with

459   50 mM 3-(*N*-morpholino) propanesulfonic acid, pH 7.0 (LB-MOPS). *Escherichia coli* was grown

460   in LB. Cultures were grown in 18-mm test tubes at a volume of 3 mL in a shaking incubator (250

461   RPM) at 37ºC. For individual colony growth we used LB supplemented with 1.5% agar. Where

462   required, broth cultures of *E. coli* and *P. aeruginosa* were supplemented with gentamicin at a

463 concentration of 10 µg per mL (Gm10). *E. coli* colonies were grown on LB supplemented with

464 1.5% agar and gentamicin at 10 µg per mL. *P. aeruginosa* colonies were grown on LB

465 supplemented with 1.5% agar and gentamicin at 100 µg per mL (Gm100) for transformations or

466 10 µg per mL for maintaining cultures.

467

468 **Construction of *P. aeruginosa* mutants.** In all experiments with the laboratory strain PAO1,

469 we used strain *P. aeruginosa* PAO1-UW (38). Clinical *P. aeruginosa* isolates were obtained from

470 the EPIC Observational Study and are from children with cystic fibrosis 5-12 years of age (34).

471 In-frame deletions of *lasR*, *pqsE*, *mexT*, and *mexEF* were generated using two-step allelic

472 exchange as previously described (39). Briefly, constructs for gene deletions were created by

473 using a pEXG2 vector backbone and Gibson assembly to 1000 bp of DNA flanking each side of

474 the gene of interest to facilitate homologous recombination. *E. coli* S17-1 was transformed with

475 each construct and used to deliver knockout plasmids to *P. aeruginosa* via conjugation.

476 Merodiploids were selected by plating on *Pseudomonas* Isolate agar containing Gm100, and

477 deletion mutants were then selected on LB agar containing 10-15% sucrose and no sodium

478 chloride. All deletion mutants were confirmed by PCR and sequencing of genomic DNA.

479

480 Overexpression constructs were created using a pUC18T mini Tn7T integrating plasmid with an

481 arabinose-inducible promoter and Gibson assembly to clone in either *pqsE* or *mexEF-oprN* CDS

482 downstream of the promoter (40). The overexpression construct was electrotransformed into *P.*

483 *aeruginosa* as described elsewhere and selected using LB supplemented with 1.5% agar and

484 gentamicin at 100 µg per mL (Gm100) (41). Proper integration at the attTn7 attachment site was

485 confirmed by PCR and sequencing of genomic DNA. Gentamicin susceptibility was restored

486 using Flp-mediated excision of gentamicin resistance marker (42).

487

488   Reporter plasmids pP*lasI*-*gfp*, pP*rhlA*-*gfp*, pP*pqsA*-*gfp,* and pP*mexE*-*gfp* were constructed in

489   pBBR1MCS-5 and contain about 200-500 bp upstream of each gene fused to *gfp*. Plasmids

490   were electrotransformed into *P. aeruginosa* as described above.

491

492   **Assays for LasR, RhlR, and PqsR activity.** To measure LasR activity, we inoculated individual

493   duplicate colonies of strains with the transcriptional reporter P*lasI*-*gfp* into LB-MOPS

494   supplemented with Gm10 and incubated at 37˚C with shaking for 18 hours. Cultures were back

495   diluted to an OD_{600} of 0.01 and grown until OD_{600} of 0.1. Exponential phase cultures were used

496   to inoculate a 48-well plate to an OD_{600} of 0.01 with a 300 μL final volume. Plates were

497   incubated at 37˚C with shaking for 18 hours in a Biotek Synergy H1 microplate reader. GFP

498   fluorescence (excitation 485 nm, emission 535 nm) and OD_{600} were measured every 20

499   minutes. The plasmids pP*rhlA*-*gfp* and pP*pqsA*-*gfp* were similarly introduced into each strain to

500   measure RhlR and PqsR activity, respectively. Where appropriate, 20 μM final PQS (in

501   methanol) was added before plates were incubated in the microplate reader. Similarly, to induce

502   *pqsE* and *mexEF-oprN* expression, LB-MOPS supplemented with Gm10 was inoculated with a

503   final concentration of 0.1% arabinose before plates were incubated in the microplate reader. All

504   experiments were performed in triplicate.

505

506   **Assay for MexT activity.** Strains were transformed with the pP*mexE*-*gfp* reporter plasmid (22).

507   Single colonies were used to inoculate LB-MOPS supplemented with Gm10 and grown for 20

508   hours. Cultures were back diluted to an OD_{600} of 0.05 in LB-MOPS supplemented with Gm10.

509   To determine whether MexT activity can be activated, 8 mM final diamide [1,1'-Azobis(N,N-

510   dimethylformamide), TCI America] was added to cultures. Cultures were incubated for 18 hours

511   at 37˚C with shaking. Endpoint GFP fluorescence (excitation 485 nm, emission 535 nm) and

512   OD_{600} were measured using a Biotek Synergy H1 microplate reader. For all endpoint

513 measurements, the background fluorescence of LB was subtracted from the final fluorescence

514 value of the reporter culture.

515

516 **RNA isolation and RNA sequencing.** Wild-type PAO1 and PAO1Δ*mexT* cultures were started

517 from single colonies in LB-MOPS in biological triplicate. Cultures were incubated for 18 hours at

518 37˚C with shaking. Cultures were back diluted to an OD_{600} of 0.1 until cultures doubled, and

519 then cultures are diluted back to an OD_{600} of 0.05. At an OD_{600} of 1.0 and 2.0, a total of an OD_{600}

520 of 2.0 was pelleted at 4000 RPM for 5 min. Supernatant was discarded and pellets were

521 resuspended in 1 mL QIAzol containing lysis beads. Samples were lysed by bead-beating at

522 maximum RPM for 1 min with chilling for 5 min. Bead-beating was repeated twice. Chloroform

523 was added, shaken vigorously, and centrifuged for 15 min at 12,000 x g at 4˚C. 450 μL of the

524 upper phase was combined with 675 μL of 100% ethanol. Samples RNA was extracted using a

525 RNeasy kit with one on-column DNase (cat. No. 79254, Qiagen) treatment, and RNA was eluted

526 using RNase-free water.

527

528 rRNA depletion, library generation, and >20 million 150-bp paired-end Illumina HiSeq reads

529 were generated for each sample commercially (Genewiz; Azenta). Trimmomatic with default

530 settings (https://github.com/timflutre/trimmomatic) was used to trim adapters prior to alignment

531 against the PAO1 reference genome (accession NC_002516) using StrandNGS version 3.3.1

532 (Strand Life Sciences, Bangalore, India). DESeq2 (27) was used for differential expression

533 analysis, using the Benjamini-Hochberg adjustment for multiple comparisons and a false-

534 discovery rate α = 0.05. Samples were grouped according to each strain and growth phase for

535 the DESeq2 differential expression analyses. MexT regulons were determined by comparing the

536 wild-type PAO1 to PAO1Δ*mexT* for a given growth phase and imposing a 2-fold minimal fold

537 change threshold. RhlR regulon genes were filtered out based on a compiled RhlR core regulon

538 (15, 16, 28). The RNA-seq data are deposited in the Gene Expression Omnibus under

539 accession number GSE291609.

540

541 **qRT PCR analysis.** RNA was extracted as described above. 200 ng total cDNA was generated

542 by reverse transcription using the qScript cDNA synthesis kit. Quantitative real-time PCR was

543 performed using 2.5 ng total cDNA using the PowerTrack SYBR Green Mix. Primers targeting

544 *mexE* were used to monitor MexT activity. Primers amplifying *rplU* were used as a

545 housekeeping gene. Data analysis was determined using relative gene expression levels using

546 $2^{-\Delta\Delta Ct}$ method.

547

548 **Measurement of C4-HSL concentrations.** Individual colonies of wild-type PAO1 or

549 PAO1Δ*mexEF* were inoculated into 3 mL LB-MOPS in triplicate. Cultures were grown at 37ºC in

550 a shaking incubator for 18 hours. Cultures were back diluted to an OD_{600} of 0.1 and grown until

551 OD_{600} of 0.2, and then back diluted to OD_{600} of 0.1. At OD_{600} of 0.3, 0.8, and 2.0, cultures were

552 removed to extract C4-HSL. To extract total C4-HSL, 3 mL of culture was transferred to an 18-

553 mm glass test tube and mixed with 3 mL acidified ethyl acetate. Samples were vortexed for 30

554 seconds and rested for 10 minutes to allow for phase separation. The clear top layer was

555 extracted to a 10 mL glass collection tube. The extraction was repeated and added to the same

556 10 mL glass collection tube. To extract extracellular C4-HSL, we first centrifuged 3 mL of culture

557 at 5000xg for 5 min and collected the supernatant in an 18 mm glass test tube and mixed with 3

558 mL acidified ethyl acetate. Samples were vortexed on high for 30 seconds and rested for 10

559 minutes to allow for phase separation. The clear top layer was extracted to a 10 mL glass

560 collection tube. The extraction was repeated and added to the same 10 mL glass collection

561 tube. For each sample, acidified ethyl acetate was evaporated using an N_2 evaporator until no

562 liquid remained. Dried fractions were resuspended in 300 µL ethyl acetate to create a 10x stock.

563

564   To measure C4-HSL, we used a bioassay strain E. coli DH5α/pEDP61.5 containing *tacp rhlR*

565   and a *rhlAB-lacZ* reporter (43). The bioassay strain was grown in 5 mL LB supplemented with

566   100 µg per mL carbenicillin for 18 hours at 37˚C with shaking. Cultures were back diluted to

567   OD_{600} of 0.05 and grown until an OD_{600} of 0.1-0.2. Cultures were induced with 1 mM final IPTG

568   and grown to OD_{600} of 0.5. C4-HSL standards and the above extracted samples were deposited

569   into 1.5 mL microcentrifuge tubes and dried with N_2. When cultures reach an OD_{600} of 0.5, 0.5

570   mL of culture was added to the prepared signal-containing tubes. Cultures were grown for 3

571   hours at 37˚C with shaking. Cultures were lysed with the addition of 50 µL chloroform, vortexed,

572   and 10 µL of the top phase of each sample was transferred to a 96-well white microtiter

573   Optiplate. Luminescence was measured using the Galacton-Plus chemiluminescent kit.

574

575

576   <u>Acknowledgements</u>

580   References

581   1.   Miller MB, Bassler BL. 2001. Quorum sensing in bacteria. Annu Rev Microbiol 55:165-
582   99.

583   2.   Schuster M, Greenberg EP. 2006. A network of networks: quorum-sensing gene
584   regulation in *Pseudomonas aeruginosa*. Int J Med Microbiol 296:73-81.

585   3.   Schuster M, Lostroh CP, Ogi T, Greenberg EP. 2003. *Identification, timin*g, and signal
586   specificity of Pseudomonas aeruginosa quorum-controlled genes: a transcriptome
587   analysis. J Bacteriol 185:2066-79.

588   4.   Fuqua WC, Winans SC, Greenberg EP. 1994. Quorum sensing in bacteria: the LuxR-
589   LuxI family of cell density-responsive transcriptional regulators. J Bacteriol 176:269-75.

590   5.   Deziel E, Lepine F, Milot S, He J, Mindrinos MN, Tompkins RG, Rahme LG. 2004.
591   Analysis of *Pseudomonas aeruginosa* 4-hydroxy-2-alkylquinolines (HAQs) reveals a role
592   for 4-hydroxy-2-heptylquinoline in cell-to-cell communication. Proc Natl Acad Sci U S A
593   101:1339-44.

594   6.   Gallagher LA, McKnight SL, Kuznetsova MS, Pesci EC, Manoil C. 2002. Functions
595   required for extracellular quinolone signaling by *Pseudomonas aeruginosa*. J Bacteriol
596   184:6472-80.

597   7.   Pesci EC, Milbank JB, Pearson JP, McKnight S, Kende AS, Greenberg EP, Iglewski BH.
598   1999. Quinolone signaling in the cell-to-cell communication system of *Pseudomonas*
599   *aeruginosa*. Proc Natl Acad Sci U S A 96:11229-34.

600   8.   Diggle SP, Cornelis P, Williams P, Camara M. 2006. 4-quinolone signalling in
601   Pseudomonas aeruginosa: old molecules, new perspectives. Int J Med Microbiol 296:83-
602   91.

603   9.   Scholz RL, Greenberg EP. 2017. Positive autoregulation of an acyl-homoserine lactone
604   quorum-sensing circuit synchronizes the population response. mBio 8.

605   10.   de Kievit TR, Kakai Y, Register JK, Pesci EC, Iglewski BH. 2002. Role of the
606   *Pseudomonas aeruginosa las* and *rhl* quorum-sensing systems in *rhlI* regulation. FEMS
607   Microbiol Lett 212:101-6.

608   11.   Sandoz KM, Mitzimberg SM, Schuster M. 2007. Social cheating in *Pseudomonas*
609   *aeruginosa* quorum sensing. Proc Natl Acad Sci U S A 104:15876-81.

610   12.   Borgert SR, Henke S, Witzgall F, Schmelz S, Zur Lage S, Hotop SK, Stephen S, Lubken
611   D, Kruger J, Gomez NO, van Ham M, Jansch L, Kalesse M, Pich A, Bronstrup M,
612   Haussler S, Blankenfeldt W. 2022. Moonlighting chaperone activity of the enzyme PqsE
613   contributes to RhlR-controlled virulence of *Pseudomonas aeruginosa*. Nat Commun
614   13:7402.

615   13.   Feathers JR, Richael EK, Simanek KA, Fromme JC, Paczkowski JE. 2022. Structure of
616   the RhlR-PqsE complex from Pseudomonas aeruginosa reveals mechanistic insights
617   into quorum-sensing gene regulation. Structure 30:1626-1636 e4.

618   14.   Brouwer S, Pustelny C, Ritter C, Klinkert B, Narberhaus F, Haussler S. 2014. The PqsR
619   and RhlR transcriptional regulators determine the level of *Pseudomonas* quinolone
620   signal synthesis in *Pseudomonas aeruginosa* by producing two different *pqsABCDE*
621   mRNA isoforms. J Bacteriol 196:4163-71.

622   15.   Asfahl KL, Smalley NE, Chang AP, Dandekar AA. 2022. Genetic and transcriptomic
623   characteristics of RhlR-dependent quorum sensing in cystic fibrosis isolates of
624   *Pseudomonas aeruginosa*. mSystems 7:e0011322.

16. Cruz RL, Asfahl KL, Van den Bossche S, Coenye T, Crabbe A, Dandekar AA. 2020. RhlR-regulated acyl-homoserine lactone quorum sensing in a cystic fibrosis isolate of *Pseudomonas aeruginosa*. mBio 11.

17. Feltner JB, Wolter DJ, Pope CE, Groleau MC, Smalley NE, Greenberg EP, Mayer-Hamblett N, Burns J, Deziel E, Hoffman LR, Dandekar AA. 2016. LasR variant cystic fibrosis isolates reveal an adaptable quorum-sensing hierarchy in *Pseudomonas aeruginosa*. mBio 7.

18. Sobel ML, Neshat S, Poole K. 2005. Mutations in PA2491 (*mexS*) promote MexT-dependent mexEF-oprN expression and multidrug resistance in a clinical strain of *Pseudomonas aeruginosa*. J Bacteriol 187:1246-53.

19. Lee S, Gallagher L, Manoil C. 2021. Reconstructing a wild-type *Pseudomonas aeruginosa* reference strain PAO1. J Bacteriol 203:e0017921.

20. Richardot C, Juarez P, Jeannot K, Patry I, Plesiat P, Llanes C. 2016. Amino acid substitutions account for most MexS alterations in clinical *nfxC* mutants of *Pseudomonas aeruginosa*. Antimicrob Agents Chemother 60:2302-10.

21. Lamarche MG, Deziel E. 2011. MexEF-OprN efflux pump exports the *Pseudomonas* quinolone signal (PQS) precursor HHQ (4-hydroxy-2-heptylquinoline). PLoS One 6:e24310.

22. Kostylev M, Smalley NE, Chao MH, Greenberg EP. 2023. Relationship of the transcription factor MexT to quorum sensing and virulence in *Pseudomonas aeruginosa*. J Bacteriol 205:e0022623.

23. Kostylev M, Kim DY, Smalley NE, Salukhe I, Greenberg EP, Dandekar AA. 2019. Evolution of the *Pseudomonas aeruginosa* quorum-sensing hierarchy. Proc Natl Acad Sci U S A 116:7027-7032.

24. Oshri RD, Zrihen KS, Shner I, Omer Bendori S, Eldar A. 2018. Selection for increased quorum-sensing cooperation in *Pseudomonas aeruginosa* through the shut-down of a drug resistance pump. ISME J 12:2458-2469.

25. Tian ZX, Fargier E, Mac Aogain M, Adams C, Wang YP, O'Gara F. 2009. Transcriptome profiling defines a novel regulon modulated by the LysR-type transcriptional regulator MexT in *Pseudomonas aeruginosa*. Nucleic Acids Res 37:7546-59.

26. Kohler T, Epp SF, Curty LK, Pechere JC. 1999. Characterization of MexT, the regulator of the MexE-MexF-OprN multidrug efflux system of *Pseudomonas aeruginosa*. J Bacteriol 181:6300-5.

27. Love MI, Huber W, Anders S. 2014. Moderated estimation of fold change and dispersion for RNA-seq data with DESeq2. Genome Biol 15:550.

28. Chugani S, Kim BS, Phattarasukol S, Brittnacher MJ, Choi SH, Harwood CS, Greenberg EP. 2012. Strain-dependent diversity in the *Pseudomonas aeruginosa* quorum-sensing regulon. Proc Natl Acad Sci U S A 109:E2823-31.

29. Kohler T, Michea-Hamzehpour M, Henze U, Gotoh N, Curty LK, Pechere JC. 1997. Characterization of MexE-MexF-OprN, a positively regulated multidrug efflux system of *Pseudomonas aeruginosa*. Mol Microbiol 23:345-54.

30. Kristensen R, Andersen JB, Rybtke M, Jansen CU, Fritz BG, Kiilerich RO, Uhd J, Bjarnsholt T, Qvortrup K, Tolker-Nielsen T, Givskov M, Jakobsen TH. 2024. Inhibition of *Pseudomonas aeruginosa* quorum sensing by chemical induction of the MexEF-oprN efflux pump. Antimicrob Agents Chemother 68:e0138723.

31. Yamaguchi A, Nakashima R, Sakurai K. 2015. Structural basis of RND-type multidrug exporters. Front Microbiol 6:327.

32. Simanek KA, Taylor IR, Richael EK, Lasek-Nesselquist E, Bassler BL, Paczkowski JE. 2022. The PqsE-RhlR interaction regulates RhlR DNA Binding to control virulence factor production in *Pseudomonas aeruginosa*. Microbiol Spectr 10:e0210821.

33. Letizia M, Mellini M, Fortuna A, Visca P, Imperi F, Leoni L, Rampioni G. 2022. PqsE expands and differentially modulates the RhlR quorum sensing regulon in *Pseudomonas aeruginosa*. Microbiol Spectr 10:e0096122.

34. Rosenfeld M, Emerson J, McNamara S, Joubran K, Retsch-Bogart G, Graff GR, Gutierrez HH, Kanga JF, Lahiri T, Noyes B, Ramsey B, Ren CL, Schechter M, Morgan W, Gibson RL, Sites ESGPC. 2010. Baseline characteristics and factors associated with nutritional and pulmonary status at enrollment in the cystic fibrosis EPIC observational cohort. Pediatr Pulmonol 45:934-44.

35. Miranda SW, Asfahl KL, Dandekar AA, Greenberg EP. 2022. *Pseudomonas aeruginosa* quorum sensing. Adv Exp Med Biol 1386:95-115.

36. Engebrecht J, Nealson K, Silverman M. 1983. Bacterial bioluminescence: isolation and genetic analysis of functions from *Vibrio fischeri*. Cell 32:773-81.

37. Le Guillouzer S, Groleau MC, Deziel E. 2017. The Complex Quorum Sensing Circuitry of Burkholderia thailandensis Is Both Hierarchically and Homeostatically Organized. mBio 8.

38. Stover CK, Pham XQ, Erwin AL, Mizoguchi SD, Warrener P, Hickey MJ, Brinkman FS, Hufnagle WO, Kowalik DJ, Lagrou M, Garber RL, Goltry L, Tolentino E, Westbrock-Wadman S, Yuan Y, Brody LL, Coulter SN, Folger KR, Kas A, Larbig K, Lim R, Smith K, Spencer D, Wong GK, Wu Z, Paulsen IT, Reizer J, Saier MH, Hancock RE, Lory S, Olson MV. 2000. Complete genome sequence of *Pseudomonas aeruginosa* PAO1, an opportunistic pathogen. Nature 406:959-64.

39. Hmelo LR, Borlee BR, Almblad H, Love ME, Randall TE, Tseng BS, Lin C, Irie Y, Storek KM, Yang JJ, Siehnel RJ, Howell PL, Singh PK, Tolker-Nielsen T, Parsek MR, Schweizer HP, Harrison JJ. 2015. Precision-engineering the *Pseudomonas aeruginosa* genome with two-step allelic exchange. Nat Protoc 10:1820-41.

40. Choi KH, Schweizer HP. 2006. mini-Tn7 insertion in bacteria with single attTn7 sites: example *Pseudomonas aeruginosa*. Nat Protoc 1:153-61.

41. Choi KH, Kumar A, Schweizer HP. 2006. A 10-min method for preparation of highly electrocompetent *Pseudomonas aeruginosa* cells: application for DNA fragment transfer between chromosomes and plasmid transformation. J Microbiol Methods 64:391-7.

42. Hoang TT, Karkhoff-Schweizer RR, Kutchma AJ, Schweizer HP. 1998. A broad-host-range Flp-FRT recombination system for site-specific excision of chromosomally-located DNA sequences: application for isolation of unmarked *Pseudomonas aeruginosa* mutants. Gene 212:77-86.

43. Pearson JP, Pesci EC, Iglewski BH. 1997. Roles of *Pseudomonas aeruginosa las* and *rhl* quorum-sensing systems in control of elastase and rhamnolipid biosynthesis genes. J Bacteriol 179:5756-67.